

Impact of Correlated Activity and STDP on Network Structure

Changan Liu^{1,2,†} and Zhong Dai³

Abstract Synaptic strengths between neurons are plastic and modified by spontaneous activity and information from the outside. There is increasing interest in the impact of correlated neuron activity and learning rules on global network structure. Here the networks of exponential integrate-and-fire neurons with spike timing-dependent plasticity (STDP) learning rules are considered, by providing the theoretical approximation of spiking cross-covariance between connected neurons and the theory for the evolution of synaptic weights. Background input mean and variance highly affect the spiking covariance, even for the fixed baseline firing rate and connection. Through analyzing the effects of covariance and STDP on vector fields for pairwise correlated neurons under fixed baseline firing rate, we show that the connections from a neuron with lower input mean to that with higher one will strengthen for balanced Hebbian STDP. However, this situation is reversed for Anti-Hebbian cases. Moreover, for potentiation dominated STDP, the synaptic weights for the networks of neurons with lower input mean are more likely to be enhanced. In addition, these properties found from coupled neurons also hold for large recurrent networks in both theories and simulations. This study provides a self-consistent theoretical method for understanding how correlated spiking activity and STDP shape the network structure and an approach for predicting structures of large networks through the analysis of simple neural circuits.

Keywords Correlated activity, network structure, phase plane, synaptic weights

MSC(2010) 37N25, 92B20.

1. Introduction

Many studies have explored how spike timing-dependent plasticity (STDP) shapes the distribution of synaptic weights of a group of synaptic connections to a single neuron [4, 23, 27, 43, 49]. Here, more challenging problems of understanding how correlated activity and STDP shape the global structure of a recurrent network of spiking neurons are considered. Related questions have been addressed before in a number of studies [8, 10, 12, 16–21, 24, 29, 32, 33, 35, 42, 45, 48, 50]. The generally

[†]the corresponding author.

Email address: changanliu@email.sdu.edu.cn (C. Liu), zhong-dai07@mail.sdu.edu.cn (Z. Dai)

¹Department of Systems Biomedicine, School of Basic Medical Sciences, Shandong University, Jinan, Shandong Province, 250012, China

²Department of Mathematics, University of Houston, Houston, TX 77204, United States

³School of Control Science and Engineering, Shandong University, Jinan, Shandong Province, 250061, China

antisymmetric shape of the STDP window, in which reversing the ordering of pre- and postsynaptic spikes reverses the direction of synaptic change, led to the proposal that this synaptic modification rule should eliminate strong recurrent connections between neurons [1, 42]. This idea has been expanded by Kozloski and Cecchi [29] to larger polysynaptic loops in the case of balanced STDP which the magnitudes of potentiation and depression are equal. The case of enhancing recurrent connections through pair-based STDP was also proposed by Song and Abbott [42] and was explored by Clopath and her colleagues [8] later in a more complex model. Clopath and her colleagues proposed a STDP model in which the synaptic changes depend on presynaptic spike arrival and the postsynaptic membrane potential. They use this model to explain the connectivity patterns in cortex with a few strong bidirectional connections. Their plasticity rule lead not only to the development of localized receptive fields but also to the connectivity patterns that reflect the neural code. An excessively active group of neurons has been shown to decouple from the rest of the network through STDP [33], and in presence of axonal delays, STDP enhances recurrent connections when the neurons fire in a tonic irregular mode [32].

Babadi and Abbott have shown that large network properties can be explained by the effect of STDP on pairwise interactions of neurons receiving Poisson input based on the baseline firing rates [5]. Gilson and his colleagues developed a theoretical framework based on the assumption that spike trains can be described as Poisson processes, and they applied this framework to analytically describe the network dynamics and the evolution of the synaptic weights in a series of five papers [16–20]. Most of these previous studies are based on the assumption that the input and output of neurons follow Poisson process, which leads to tractable models and frameworks. However, such strong assumption does not fully reflect a number of properties of actual neurons. One of the main issues is the background noisy input in neuronal firing, although the Poisson model captures such input indirectly through the probabilistic nature of the firing of spikes. So it can not provide a mechanistic explanation of neuronal response variability. Poisson-like spike generation, by itself, is highly reliable and deterministic. However, background input in neural responses is believed to result in part from the fact that synapses are very unreliable [2]. Background input is therefore due to unreliable synapses, or inherited from the input from the rest of the network, and is not due to spike generation. For the integrate-and-fire neuron model, the output is a filtered, thresholded and deterministic function of the input. Thus, such model captures many of the qualitative features, and is often applied as a starting point for conceptualizing the biophysical behavior of single neurons [44].

There is evidence showing that actual neurons respond as integrate-and-fire neurons [37] through biological experiments, which implies such neuron models are closer to the real ones. Here the networks built of the general type of integrate-and-fire neurons: exponential integrate-and-fire (EIF) neurons [13] are considered, which have been shown to match spiking dynamics well in certain cortical areas [6]. In this paper, how correlated spiking activity and STDP affect the evolution of network structure under the same fixed baseline firing rate is illustrated, which may not be captured by following the assumption of Poisson-like neurons.

2. Methods

2.1. Network neuron model

All the networks we considered here are composed of exponential integrate-and-fire (EIF) neurons. The membrane potential (voltage) V_i of neuron i in a network is modeled by

$$C_m \frac{dV_i}{dt} = g_L(V_L - V_i) + g_L\psi(V_i) + I_i(t) + f_i(t). \quad (2.1)$$

Here C_m is the membrane capacitance, V_L is the leak reversal potential, and g_L is the membrane conductance.

$$\psi(V_i) = \Delta_T \exp\left[\frac{V_i - V_T}{\Delta_T}\right]$$

is the exponential term. V_T is the initiation threshold and Δ_T shapes the spiking dynamics of the membrane potential. An action potential (spike) will be generated when the membrane potential reaches V_T . In numerical simulations, a threshold V_{th} is set up for making action potentials. After an action potential is generated, the membrane potential is reset to the rest potential V_{re} and is held there for an absolute refractory period τ_{ref} .

In vivo, neurons are not isolated and they function in a complex environment. So they are affected by internal inputs due to channel noise [51] and external inputs which are not explicitly modelled [38]. As a result, these two parts are modeled together as a Gaussian white noise process, the background input term: $I_i(t) = \mu_i + g_L\sigma_i D\xi_i(t)$. μ_i is the mean of the input and σ_i governs the noise strength. $D = \sqrt{\frac{2C_m}{g_L}}$ controls the noise amplitude to be independent of the passive membrane time constant. The reason why the EIF neuron model is applied to build networks is that it can accurately predict the statistical features of spike trains for a large class of neurons, such as pyramidal neurons [26].

A post-synaptic input current is generated whenever a presynaptic cell spikes. The synaptic kernels are assumed to be exponential, and thus we have the form:

$$\mathbf{J}_{ij}(t) = \mathbf{W}_{ij}\mathcal{H}(t - \tau_D)\exp\left[-\frac{t - \tau_D}{\tau_S}\right].$$

Here \mathcal{H} is the heaviside step function, τ_D is the synaptic delay, and τ_S is the synaptic time constant. The matrix \mathbf{W} defines the synaptic weights for all the connections in a network, and the entry \mathbf{W}_{ij} denotes the synaptic weight of the directed connection from neuron j to neuron i . $y_j(t) = \sum_k \delta(t - t_{j,k})$ is the output spike train of neuron j . Then the post-synaptic input current for neuron i generated by the spike train of neuron j is given by $f_i(t) = \sum_j (\mathbf{J}_{ij} * y_j)(t)$.

2.2. The STDP learning rule

To study how plasticity shapes the structure of the network, a well-known model of Hebbian spike timing-dependent plasticity (STDP) [15] rule is applied, which was supported by experimental evidence from Bi and Poo in 1998 [7] and other

studies [3, 25, 52]. If the time difference between the pre- and post-synaptic spikes is denoted by s :

$$s = t_{post} - t_{pre} = t_j - t_i ,$$

then a Hebbian STDP rule is defined by

$$\Delta \mathbf{W}_{ji}(s) = \begin{cases} \mathbf{W}_{ji}^0 \mathcal{H}(W^{max} - \mathbf{W}_{ji})L(s) , & \text{if } s \geq 0 \\ \mathbf{W}_{ji}^0 \mathcal{H}(\mathbf{W}_{ji})L(s) , & \text{if } s < 0 \end{cases} , \quad (2.2)$$

where

$$L(s) = \begin{cases} f_+ e^{-\frac{|s|}{\tau_+}} , & \text{if } s \geq 0 \\ -f_- e^{-\frac{|s|}{\tau_-}} , & \text{if } s < 0 \end{cases} .$$

Here \mathcal{H} is also the Heaviside function, $f_+ > 0$ and $f_- > 0$ are the amplitudes of potentiation and depression respectively, τ_+ and τ_- are the time constants, W^{max} is the upper bound of the synaptic weights and \mathbf{W}^0 is the binary adjacency matrix of the network, enforcing that the STDP rule can only modify connections that exist in the network structure.

The Anti-Hebbian STDP rule is also considered, which is defined by the following function:

$$\Delta \mathbf{W}_{ji}(s) = \begin{cases} \mathbf{W}_{ji}^0 \mathcal{H}(\mathbf{W}_{ji})L(s) , & \text{if } s \geq 0 \\ \mathbf{W}_{ji}^0 \mathcal{H}(W^{max} - \mathbf{W}_{ji})L(s) , & \text{if } s < 0 \end{cases} ,$$

where

$$L(s) = \begin{cases} -f_- e^{-\frac{|s|}{\tau_+}} , & \text{if } s \geq 0 \\ f_+ e^{-\frac{|s|}{\tau_-}} , & \text{if } s < 0 \end{cases} .$$

We can see that this rule is similar to the Hebbian STDP rule defined in Eq (2.2), but with reversed windows of potentiation and depression.

2.3. Approximation of cross-covariances by linear-response theory

Here we briefly introduce the approximation method applied to estimate the pairwise spike train cross-covariances $\mathbf{C}_{ij}(s)$ for coupled neurons in a network using a synaptic weight matrix \mathbf{W} [11, 31, 34, 47]. The Fourier transform of the spike train (Eq. (2.5)) is

$$\tilde{\mathbf{y}}_i(\omega) = \int_{-\infty}^{\infty} \mathbf{y}_i(t) e^{-2\pi i \omega t} dt ,$$

where ω is the frequency. Assuming the synaptic weights \mathbf{W}_{ij} are weak, the spike response for neuron i (Eq. (2.1)) can be approximated as

$$\tilde{\mathbf{y}}_i(\omega) \approx \tilde{\mathbf{y}}_i^0(\omega) + \tilde{A}_i(\omega) \left(\sum_{j=1}^N \tilde{\mathbf{J}}_{ij}(\omega) \tilde{\mathbf{y}}_j(\omega) \right) . \quad (2.3)$$

Here $\tilde{A}_i(\omega)$ is the Fourier transform of the linear response [14] of the post-synaptic neuron i , measuring how strongly modulations in synaptic currents at frequency ω are transferred into modulations of instantaneous firing rate about a background state $\tilde{\mathbf{y}}_i^0(\omega)$. $\tilde{A}_i(\omega)$ can be computed by standard methods based on using a Fokker-Planck equation [39, 40], which describes the probability distribution of a neuron's membrane potential. The function $\tilde{\mathbf{J}}_{ij}(\omega)$ is the Fourier transform of a synaptic filter. Eq. (2.3) is a linear approximation for how a neuron integrates and transforms a realization of synaptic input into a spike train.

Following the works [11, 31, 47] and applying this linear approximation to estimate the Fourier transform of $\mathbf{C}_{ij}(s)$, which can be written as

$$\tilde{\mathbf{C}}_{ij}(\omega) = \langle \tilde{\mathbf{y}}_i(\omega) \tilde{\mathbf{y}}_j^*(\omega) \rangle .$$

Here $\tilde{\mathbf{y}}^*$ denotes the conjugate transpose and $\langle \cdot \rangle$ denotes the trial average. This yields the following matrix form

$$\tilde{\mathbf{C}}(\omega) \approx (\mathbf{I} - \tilde{\mathbf{K}}(\omega))^{-1} \tilde{\mathbf{C}}^0(\omega) (\mathbf{I} - \tilde{\mathbf{K}}^*(\omega))^{-1} , \quad (2.4)$$

where $\tilde{\mathbf{K}}(\omega)$ is an interaction matrix defined by $\tilde{\mathbf{K}}_{ij}(\omega) = \tilde{A}_i(\omega) \tilde{\mathbf{J}}_{ij}(\omega)$. The diagonal matrix $\tilde{\mathbf{C}}^0(\omega)$ is the auto-spectra in the absence of synaptic coupling, with elements $\tilde{\mathbf{C}}_{ii}^0(\omega) = \langle \tilde{\mathbf{y}}_i^0(\omega) \tilde{\mathbf{y}}_i^{0*}(\omega) \rangle$. \mathbf{I} is the identity matrix. From Eq. (2.4), we can recover the spiking cross-covariance matrix $\mathbf{C}(s)$ through inverse Fourier transformation. Thus, Eq. (2.4) gives us an estimate of the statistics of pairwise spiking activity in the full network given by its architecture. The process of approximating the cross-covariance for a simple two-cell network with just one connection is demonstrated in Fig. (1).

2.4. Dynamics for synaptic weights modification

The spiking output (spike train) of a neuron i is denoted by

$$\mathbf{y}_i(t) = \sum_{i=1}^{n_i} \delta(t - t_i) , \quad (2.5)$$

where $\delta(t - t_i)$ is the Dirac Delta function

$$\delta(t - t_i) = \begin{cases} \infty , & t = t_i \\ 0 , & \text{otherwise} \end{cases} .$$

According to [1, 4, 21, 28], the bridge from the joint statistics of $\mathbf{y}_i(t)$ and $\mathbf{y}_j(t)$ to the evolution of synaptic weights can be built. The STDP rule given in Eq. (2.2) governs the modification of the synaptic weight \mathbf{W}_{ji} (from neuron i to neuron j). Let $\Delta_T \mathbf{W}_{ji}$ be the total change in the related synaptic weight during a time interval of length T . This weight change is calculated by summing the contributions of input (i) and output (j) spikes occurring in the time interval $[t, t + T]$. This yields

$$\Delta_T \mathbf{W}_{ji} = \int_t^{t+T} \int_t^{t+T} \Delta \mathbf{W}_{ji}(t_2 - t_1) \mathbf{y}_j(t_2) \mathbf{y}_i(t_1) dt_2 dt_1 .$$

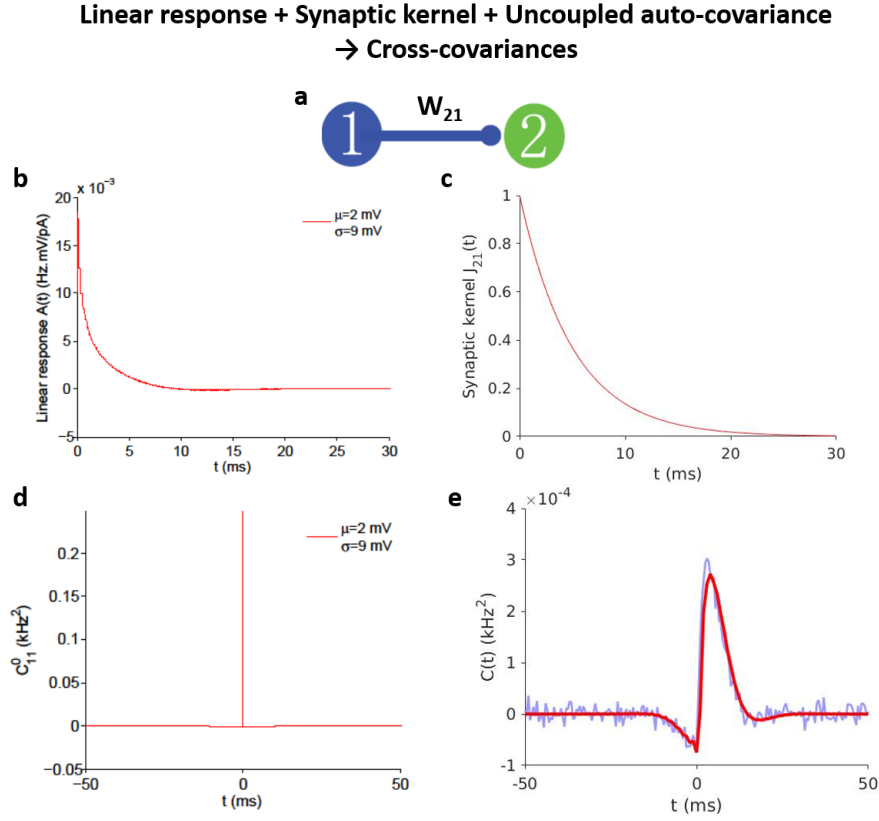


Figure 1. The process of approximating the spiking cross-covariance theoretically. The baseline firing rate is about 27 Hz for the neurons with $\mu = 2$ mV and $\sigma = 9$ mV. Here $\mathbf{W}_{21} = 1 \mu\text{A}/\text{cm}^2$. (a) The illustration of the simple two-cell network with just one directed connection from neuron 1 to neuron 2. (b) The linear response function, $A_2(t)$. (c) The synaptic kernel, $J_{21}(t)$. (d) The auto-covariance for uncoupled neuron 1, C_{11}^0 . (e) The cross-covariance $C_{21}(t)$. The smooth red curve is the theoretical approximation, while the jagged blue curve is the simulated realization. Here we use the spike trains with time length of 10^7 ms and bin size of 0.5 ms for computing the numerical cross-covariance.

Let $s = t_2 - t_1$ and $\langle \cdot \rangle$ denote the trial average. Then the trial-averaged rate of synaptic weight change is

$$\frac{\langle \Delta_T \mathbf{W}_{ji} \rangle}{T} = \frac{1}{T} \int_t^{t+T} \int_{t-t_1}^{t+T-t_1} \Delta \mathbf{W}_{ji}(s) \langle \mathbf{y}_j(t_1 + s) \mathbf{y}_i(t_1) \rangle ds dt_1 .$$

In addition, the trial-averaged spike train cross-covariance $\mathbf{C}_{ji}(s)$ is

$$\begin{aligned} \mathbf{C}_{ji}(s) &= \mathbf{E}[(\mathbf{y}_j(t_1 + s) - r_j)(\mathbf{y}_i(t_1) - r_i)] \\ &= \mathbf{E}[\mathbf{y}_j(t_1 + s) \mathbf{y}_i(t_1)] - r_i r_j \\ &= \frac{1}{T} \int_t^{t+T} \langle \mathbf{y}_j(t_1 + s) \mathbf{y}_i(t_1) \rangle dt_1 - r_i r_j , \end{aligned}$$

where \mathbf{E} is the expectation operator while r_j and r_i are the stationary firing rates

for neuron j and i respectively. Applying this term into Eq. (2.6), we have

$$\frac{\langle \Delta_T \mathbf{W}_{ji} \rangle}{T} = \int_{t-t_1}^{t+T-t_1} \Delta \mathbf{W}_{ji}(s) (\mathbf{C}_{ji}(s) + r_j r_i) ds . \quad (2.6)$$

Here the width of the learning rule $\Delta \mathbf{W}_{ji}(s)$ is defined by \mathcal{W} and let $T \gg \mathcal{W}$. Then most of the contributions to the weights evolution of the learning rule should be inside the interval $[-\mathcal{W}, \mathcal{W}]$. Thus, the integration over s in Eq. (2.6) can be extended to go over from $-\infty$ to $+\infty$. The amplitude of individual changes in the synaptic weights is required to be small ($f_{\pm} \ll W^{max}$). So the value of \mathbf{W}_{ji} does not change much in the time interval of length T . Thus T separates the time scale \mathcal{W} from the time scale of the learning dynamics, which allows us to approximate the left-hand side of Eq. (2.6) by the rate of change $\frac{d\mathbf{W}_{ji}}{dt}$

$$\begin{aligned} \frac{d\mathbf{W}_{ji}}{dt} &= \int_{-\infty}^{+\infty} \Delta \mathbf{W}_{ji}(s) (\mathbf{C}_{ji}(s) + r_j r_i) ds \\ &= \underbrace{\int_{-\infty}^{+\infty} \Delta \mathbf{W}_{ji}(s) \mathbf{C}_{ji}(s) ds}_1 + r_j r_i \underbrace{\int_{-\infty}^{+\infty} \Delta \mathbf{W}_{ji}(s) ds}_2 . \end{aligned} \quad (2.7)$$

For the fixed learning rule and neuron properties of the networks, part 2 of Eq. (2.7) is a constant. Part 1 is illustrated in Fig. 2. The process of obtaining the theoretical synaptic weight evolution is demonstrated in Fig. 3 for a simple two-cell network (Fig. 1a).

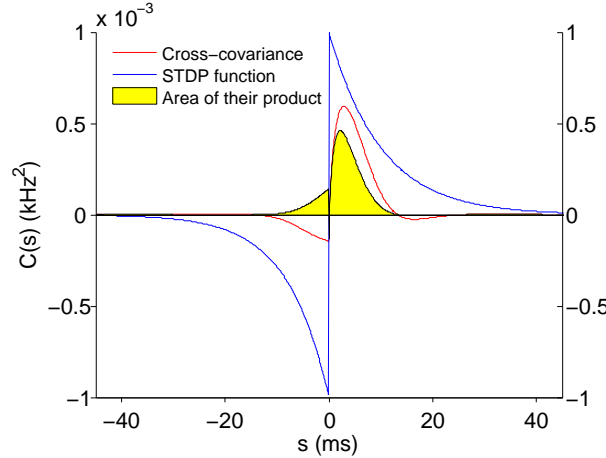


Figure 2. Illustration for Part 1 of Eq. (2.7). Cross-covariance (red curve), together with the STDP rule (blue curve) define the weight change dynamics (yellow region). These terms are calculated to obtain the theoretical weight change dynamics. The yellow region is the integral (area) of the product of cross-covariance and learning rule, which stands for Part 1 of Eq. (2.7). It contributes to the evolution of synaptic weights.

2.5. Numerical simulations

Simulations were coded in MATLAB and C++. The stochastic differential equations were discretized by a standard Euler method with a time-step of 0.01 ms.

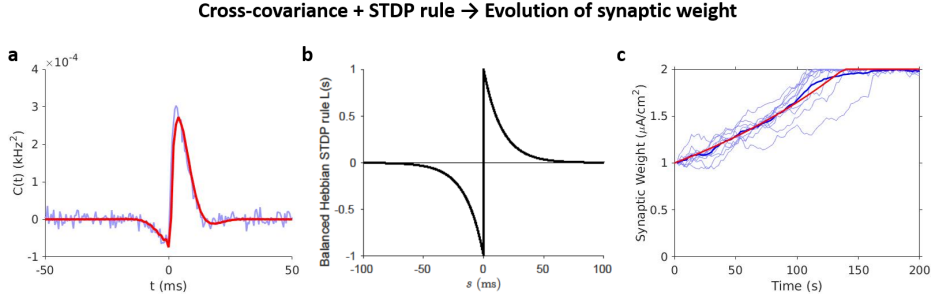


Figure 3. The process of approximating the evolution of synaptic weight theoretically. The baseline firing rate is about 27 Hz for the two neurons with $\mu = 2$ mV and $\sigma = 9$ mV. (a) Cross-covariance $C_{21}(t)$, the same as Fig. 1e. (b) Balanced Hebbian STDP rule for the network (Fig. 1a). (c) The evolution of the synaptic weight W_{21} under such STDP rule. The smooth red curve is the theoretical approximation. The 10 jagged shallow blue curves are simulated realizations, and the jagged deep blue curve is their average.

General parameter values were as follows: $C_m = 1 \mu\text{F}/\text{cm}^2$, $g_L = 0.1 \text{ mS}/\text{cm}^2$, $V_L = -72 \text{ mV}$, $\Delta_T = 1.4 \text{ mV}$, $V_T = -48 \text{ mV}$, $V_{th} = 30 \text{ mV}$, $V_{re} = -72 \text{ mV}$, $\tau_{ref} = 2 \text{ ms}$, $\tau_S = 5 \text{ ms}$, $\tau_D = 1 \text{ ms}$, $\tau_+ = \tau_- = 15$, $f_+ = f_- = W^{max}/5000$ (for balanced STDP). The specified parameters are mentioned in this manuscript.

3. Results

For studying the impact of correlated spiking activity and STDP on the evolution of network structure, the linear response theory (see Section 2.3) is applied to approximate the spiking cross-covariance between coupled neurons in the network. It is essential that the synaptic weights of the connections between neurons are required to change slowly compared with network dynamics, which provides a separation of time scales. This allows us to determine how the synaptic weights evolve. The approach described in [47] is generalized with the STDP rule to analyze the vector fields (or phase planes) of synaptic weights for two-cell recurrent networks. Then the properties found for simple neuron circuits were applied to predict the evolution of structures for large networks. Moreover, our theoretical framework matches with direct numerical simulations.

3.1. Different background input can attain the same firing rate

The Poisson-like neuron is completely described by its firing rate [41]. However, the dynamics and response of the EIF neuron are governed by parameters that can capture much more physiological properties of actual neurons. Here we focus on two parameters governing the background input, the mean μ and σ which controls noise variance. Both of them affect the firing rate and the output variability of neurons [30]. Although the same baseline firing rate (for isolated neurons) can be achieved for different μ and σ values (Fig. 4), the variability of the output is different. The statistics of the output spike trains varies according to the μ and σ

values (Fig. 5), even for the same fixed baseline firing rate. EIF neurons with higher μ (lower σ) generate more regular spike trains (Fig. 5b) than those with lower one (Fig. 5c). Moreover, coefficient of variation (CV) of the background input can vary even if the firing rate stays the same.

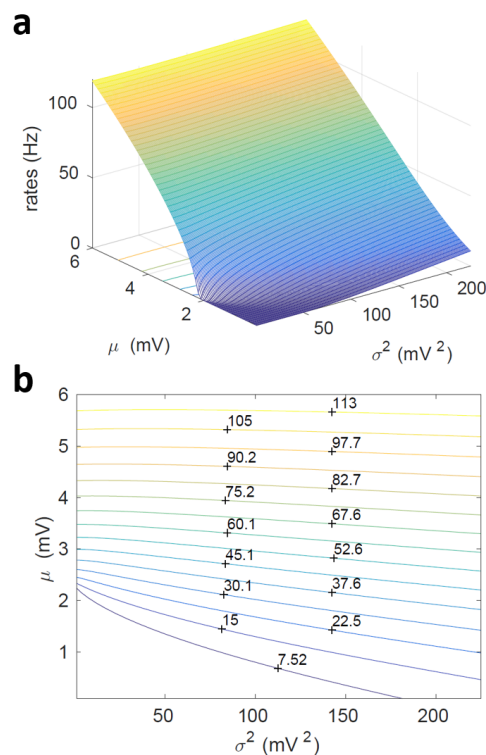


Figure 4. Different μ - σ values can attain the same baseline firing rate. (a) Changes of baseline firing rate according to μ and σ values. **(b)** Bottom of (a), illustrating that different μ and σ values can attain the same baseline firing rate. The values near to the lines are baseline firing rate.

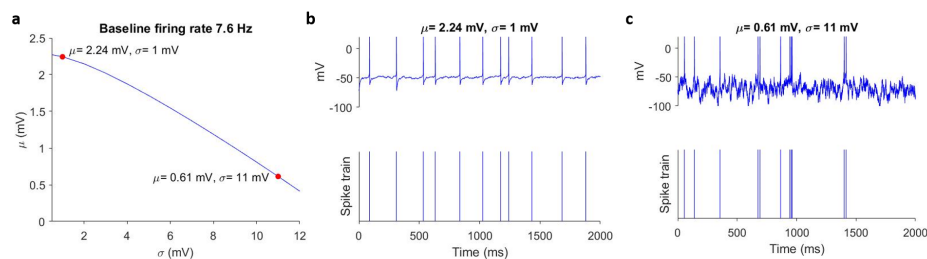


Figure 5. Neurons with the same baseline firing rate can have different firing statistics. (a) Different μ and σ values can attain the same baseline firing rate 7.6 Hz by fixing other parameters. Here I choose two μ - σ pairs: one with higher μ value while the other with lower one. **(b)** The selected EIF neuron with higher μ value (lower σ value) generates regular spike train. **(c)** The selected EIF neuron with lower μ value (higher σ value) generates irregular spike train.

Fixing other parameters, five different μ - σ pairs (Table 1) can lead to the same baseline firing rate 7.6 Hz. For fixed baseline firing rate, the value of μ decreases when increasing σ value. The reversed setting is similar. The μ - σ pairs showed in the table are applied to study the effect of their spiking covariance on network structures with the STDP rule. Besides background input mean μ and σ for noise variance, other parameters can also affect the firing rates, such as the spiking dynamics shaping parameter Δ_T in the exponential term $\psi(V_i)$ (Eq. (2.1)). Higher Δ_T causes more rapid spike onset, and leads to higher firing rates. However, the impact of these parameters is expected to be small compared to μ and σ . So here only μ and σ in the background input term are considered.

Table 1. Five different μ - σ pairs that attain the same baseline firing rate 7.6 Hz.

Pair index	μ (mV)	σ (mV)	Fano factor	Baseline firing rate (Hz)
1	1.37	7	0.77	7.6
2	1.19	8	0.81	
3	1.00	9	0.84	
4	0.81	10	0.88	
5	0.61	11	0.91	

3.2. Background input affects correlated activity and synaptic weights evolution with STDP

In addition to the STDP rule, spiking covariance also contributes to the evolution of synaptic weights in networks (Eq. (2.7)). Begin with the simple two-cell recurrent networks (Fig. 6a) with fixed baseline firing rate for both neurons, two cases are illustrated here: one of the identical neurons with higher μ value (lower σ value) while the other of identical neurons with lower μ value (higher σ value). The spiking cross-covariance for the network of neurons with higher μ value has bigger amplitude (Fig. 6e) than that with lower μ value (Fig. 6c). The reason is that higher background input mean makes neurons more sensitive to its input. The balanced ($f_+ = f_-$ and $\tau_+ = \tau_-$) Hebbian STDP rule (Fig. 6b) is applied for these two cases. Under such an STDP rule, the evolution of the synaptic weights for the network of neurons with higher μ value (lower σ value) is faster (Fig. 6f) than that with lower one (Fig. 6d), which is caused by their different cross-covariances.

According to Eq. (2.7), only the first part contains the spiking cross-variance. So the cross-variance will dominate the evolution of network structure if the contribution of the second part can be ignored. This implies

$$\begin{aligned}
 & r_i r_j \int_{-\infty}^{+\infty} \Delta \mathbf{W}_{ji}(s) ds \\
 &= r_i r_j \left(f_+ \int_0^{+\infty} e^{-\frac{s}{\tau_+}} ds - f_- \int_{-\infty}^0 e^{\frac{s}{\tau_-}} ds \right) \\
 &= r_i r_j (f_+ \tau_+ - f_- \tau_-) = 0 .
 \end{aligned}$$

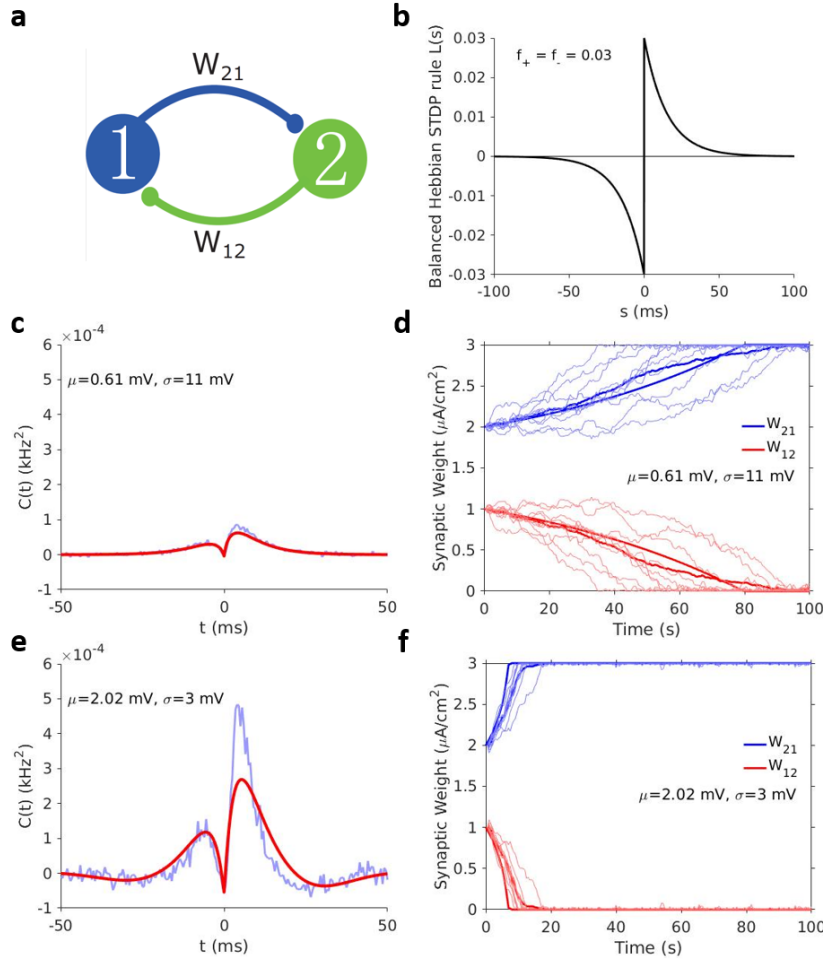


Figure 6. Synaptic weights evolution in two-cell recurrent networks with different μ - σ settings but the same baseline firing rate. Here I fix other parameters and the baseline firing rate as 7.6 Hz. **(a)** The illustration of the two-cell recurrent network. **(b)** The selected balanced Hebbian STDP rule. **(c)** Cross-covariance C_{21} for network of neurons with lower μ value. Smooth red curve is the theoretical approximation while the blue one is from numerical simulation. **(d)** The evolution of the two synaptic weights in the network of neurons with lower μ value. The smooth curves are obtained from theory. Each of the shallow jagged curves comes from one numerical simulation. The deep jagged curves are their average (10 simulated results), respectively. **(e)** Cross-covariance C_{21} for network of neurons with higher μ value. **(f)** The evolution of the two synaptic weights in the network of neurons with higher μ value.

Since the baseline firing rates can not be 0 for alive neurons, the correlated spiking activity will dominate the changes of synaptic weights in a network when $f_+ \tau_+ = f_- \tau_-$ for the STDP rule. The balanced STDP just follows this scenario.

3.3. Networks of neurons with different background input

Here the phase planes (or vector fields) for two-cell recurrent networks (Fig. 6a) of neurons with different background input but the same baseline firing rate (Table 1) are analyzed, which are inspired by the idea from Babadi and Abbott [5]. According

to Eq. (2.7), the evolution of the two synaptic weights for such a network is governed by the following system of differential equations:

$$\begin{cases} \frac{d\mathbf{W}_{12}}{dt} = \int_{-\infty}^{+\infty} \Delta\mathbf{W}_{12}(s)(\mathbf{C}_{12}(s) + r_1r_2)ds \\ \frac{d\mathbf{W}_{21}}{dt} = \int_{-\infty}^{+\infty} \Delta\mathbf{W}_{21}(s)(\mathbf{C}_{21}(s) + r_2r_1)ds \end{cases}.$$

Given an initial value of the paired synaptic weights $(\mathbf{W}_{12}, \mathbf{W}_{21})$, the corresponding phase plane shows what values will $(\mathbf{W}_{12}, \mathbf{W}_{21})$ attain under certain learning rule. Here the same balanced STDP rule is applied to these networks.

3.3.1. Hebbian case

For the network of identical neurons, its phase plane is symmetric (Fig. 7a) under balanced Hebbian STDP rule. The red diagonal consists of unstable equilibria. There are two stable fixed points $(\mathbf{W}_{21}, \mathbf{W}_{12})=(5,0)$ and $(\mathbf{W}_{21}, \mathbf{W}_{12})=(0,5)$ with symmetric basins of attraction, which means their attracting abilities are equal. This is due to the balanced learning rule. We can therefore predict that, for a big network of identical neurons under balanced Hebbian STDP, if the initial synaptic weights are uniformly distributed (follows $U(0, W^{max})$), then half of the weights will be potentiated while the other half will be depressed.

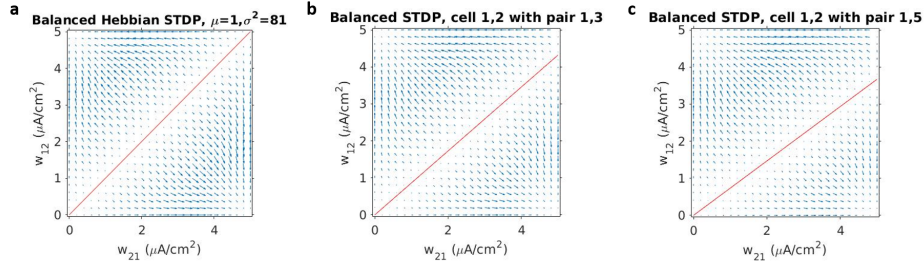


Figure 7. Phase planes for synaptic weights in two-cell recurrent networks under balanced Hebbian STDP. Here we apply the parameter settings $(\mu\text{-}\sigma)$ pairs in Table 1. We set the upper bound of all the synaptic weights to $W^{max} = 5 \mu\text{A}/\text{cm}^2$. (a) Phase plane for identical neurons with parameter setting 3. (b) Phase plane for neuron 1 with parameter setting 1 while neuron 2 with parameter setting 3. (c) Phase plane for neuron 1 with parameter setting 1 while neuron 2 with parameter setting 5.

The symmetry of the phase plane will not hold when the two neurons have different parameter settings (Fig. 7b and c). The line of unstable fixed points is tilted toward the axis corresponding to the synaptic weight \mathbf{W}_{21} , the strength of the connection from neuron with higher drive (μ) to that with lower one (from neuron 1 to neuron 2). This implies that the basin of attraction for the fixed point $(\mathbf{W}_{21}, \mathbf{W}_{12})=(0,5)$ is larger than that for $(\mathbf{W}_{21}, \mathbf{W}_{12})=(5,0)$. The outgoing synapse (\mathbf{W}_{12}) of the neuron with lower mean input (neuron 2) are more likely to be potentiated, while its incoming synapse (\mathbf{W}_{21}) are likely to weaken. For neuron with higher μ value (neuron 1), it has the opposite property. Moreover, bigger difference between the mean input values (μ) of the two neurons makes this tendency more obvious. So we can make a prediction that, for a large network of different groups of neurons with the same baseline firing rate but different background input, under balanced Hebbian STDP rule, if all the initial synaptic weights are uniformly

distributed, then the connections from the groups of neurons with lower background input mean (μ) to those with higher one are more likely to strengthen. In the meanwhile, the reversed connections are more likely to weaken. This prediction will be verified in the following illustration.

Here a network of 100 neurons with all-to-all connectivity is considered. The initial synaptic weights of the connections are uniformly distributed (Fig. 8). These 100 neurons are divided into two groups with even number of cells: group 1 (neuron 1-50) with parameter setting 3 (lower μ , higher σ , Table 1) while group 2 (neuron 51-100) with parameter setting 1 (higher μ , lower σ). This makes sure that all the 100 neurons have the same baseline firing rate, but different background input for different groups. Under such setup, we can split the synaptic weight matrix into four quarters corresponding to connections within and between these two groups. A balanced Hebbian STDP rule is applied to this network.

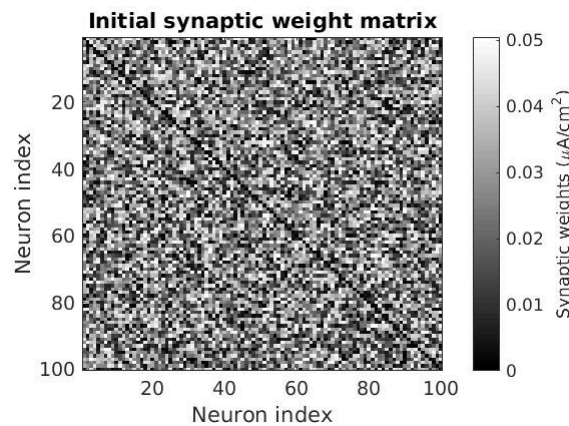


Figure 8. The initial synaptic weight matrix of the 100-cell network.

The synaptic weight matrices for the final state of the network after training from both theory and simulations are shown in Fig. 9. What's more, we record the evolution of every connection in the network (Fig. 10). We can see that the results from theory and simulated realizations are consistent. The bottom-left quarter of the final synaptic weight matrices (Fig. 9), which contains the synaptic weights of the connections from group 1 neurons (with lower μ) to group 2 neurons (with higher μ), is lighter than the top-right quarter with connections from group 2 neurons to group 1 neurons. This means there are more potentiated weights in the bottom-left quarter. In addition, the brightness of top-left quarter and bottom-right quarter, which contains the weights of the connections between neurons within the same group, are on the same level. Next, the means of the synaptic weights for each of the four quarters are calculated (Table 2) to quantify their differences. We can see that the mean of the synaptic weights for bottom-left quarter is bigger than that for top-right quarter indeed for both theory and simulations. The means of the weights for the rest two quarters are the same. These imply that the theoretical results match with the simulations.

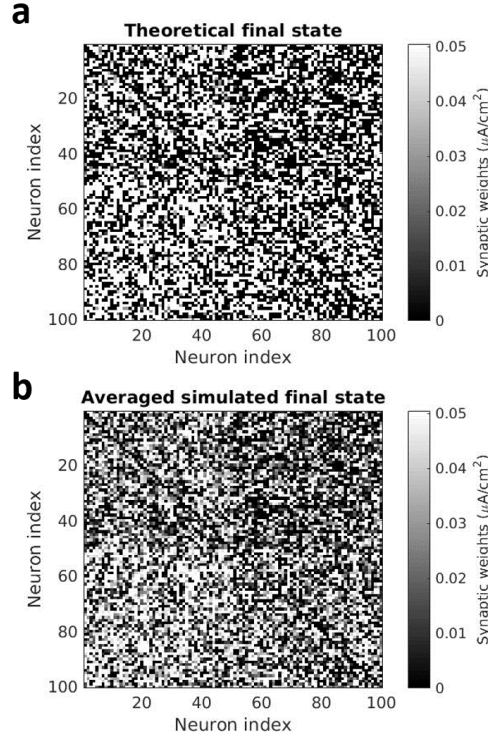


Figure 9. The synaptic weight matrices for the final state of the network under balanced Hebbian STDP. (a) The synaptic weight matrix for the final state obtained by theory. (b) The synaptic weight matrix for the final state obtained by averaging 10 numerical simulations.

Table 2. The mean of the synaptic weights in each of the four quarters for Fig. 9.

group 1: pair 3(lower μ) group 2: pair 1(higher μ)	mean weights($\mu\text{A}/\text{cm}^2$)		standard error
	theory	simulation	
lower \rightarrow lower(top-left)	0.025	0.025	0.00039
higher \rightarrow lower(top-right)	0.020	0.020	0.00040
lower \rightarrow higher(bottom-left)	0.030	0.030	0.00039
higher \rightarrow higher(bottom-right)	0.025	0.025	0.00040

3.3.2. Anti-Hebbian case

The effect of balanced Anti-Hebbian STDP rule (see Section 2.2) is also explored on the evolution of network structure. Similar to the balanced Hebbian case, the phase planes for two-cell recurrent networks following the same neuron setting are analyzed firstly as Hebbian case.

Since the difference between Anti-Hebbian STDP and Hebbian STDP is the reversal of potentiation side and depression side, similar phase planes are obtained (Fig. 11), but with reversed time flow (the direction of arrows). Here the red line

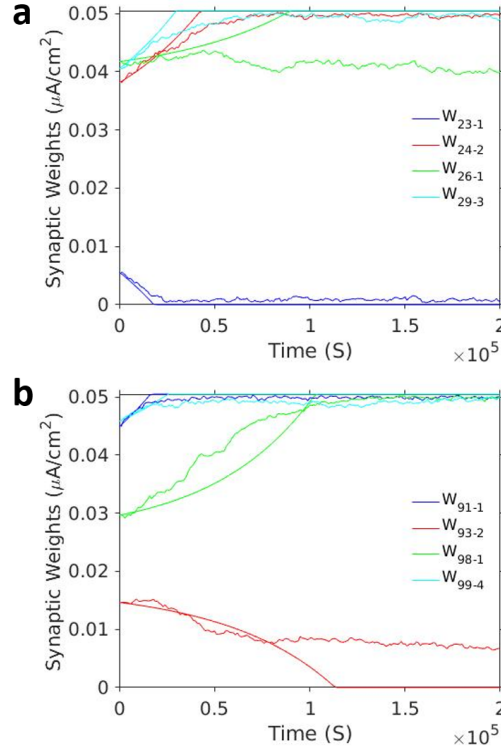


Figure 10. The evolution of selected synaptic weights in the 100-cell network under balanced Hebbian STDP. Corresponding to Fig. 9. (a, b) The smooth curves are got from theory, while the jagged curves are obtained by averaging 10 simulated realizations.

is composed of stable fixed points, where $(\mathbf{W}_{21}, \mathbf{W}_{12}) = (5, 0)$ and $(\mathbf{W}_{21}, \mathbf{W}_{12}) = (0, 5)$ become unstable fixed points. For identical neurons, the phase plane is also symmetric (Fig. 11a). All the initial synaptic weights are attracted by the diagonal. Thus, we can therefore predict that, for a large network of identical neurons under balanced Anti-Hebbian STDP, all the synaptic weights will attain similar values eventually if the initial synaptic weights are uniformly distributed.

As the two neurons have different background inputs, the line of stable fixed points is also tilted toward the axis corresponding to the synaptic weight \mathbf{W}_{21} (Fig. 11b and c), which is the same as Hebbian case. However, this implies that the outgoing synapse (\mathbf{W}_{12}) of the neuron with lower mean input (neuron 2) are more likely to weaken, while its incoming synapse (\mathbf{W}_{21}) is likely to be potentiated. The opposite property holds for neuron with higher μ value (neuron 1). As a result, we can predict that, for a large network of different groups of neurons with the same baseline firing rate but different background input, under balanced Anti-Hebbian STDP rule, the connections from the groups of neurons with lower background input mean (μ) to those with higher one are more likely to weaken if the initial synaptic weights are uniformly distributed, while the reversed connections are more likely to strengthen.

Here a network of 100 neurons with the same initial synaptic weight matrix is considered as Hebbian case (Fig. 8). These 100 neurons are divided into two

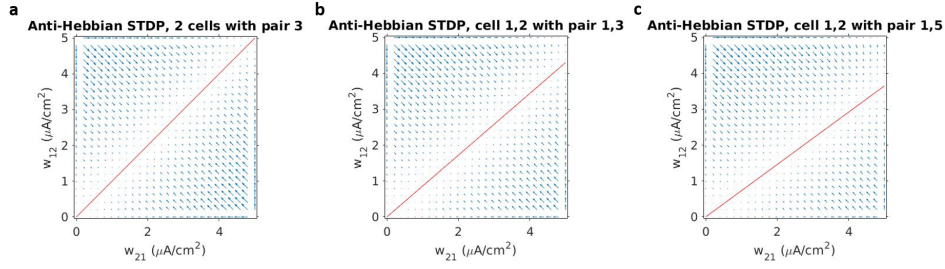


Figure 11. Phase planes for synaptic weights in two-cell recurrent networks under balanced Anti-Hebbian STDP rule. Here the parameter settings are the same as Fig. 7 except the STDP rule. (a) Phase plane for identical neurons with parameter setting 3. (b) Phase plane for neuron 1 with parameter setting 1 while neuron 2 with parameter setting 3. (c) Phase plane for neuron 1 with parameter setting 1 while neuron 2 with parameter setting 5.

even groups. We set group 1 neurons with parameter setting 1 (higher μ , lower σ , Table 1) while group 2 neurons with parameter setting 5 (lower μ , higher σ). Then balanced Anti-Hebbian STDP rule is applied to this network.

The synaptic weight matrices after training are in Fig. 12 and the selected evolution of synaptic weights are shown in Fig. 13. We have the similar pattern of four quarters to Hebbian case. Here the bottom-left quarter is also lighter than the top-right quarter. However, the former contains the synaptic weights of the connections from neurons with higher μ (group 1 neurons) to neurons with lower μ (group 2 neurons) while the latter contains the weights for the reversed connections. This is due to the reversal of potentiation side and depression side compared with Hebbian case. After calculating the means of the synaptic weights for each quarter (Table 3), we can see the mean of the synaptic weights for bottom-left quarter is bigger than that for top-right quarter while the means of the weights for the rest two quarters are the same. The mean values got from theory and simulations for each quarter are identical, which verifies our prediction.

Table 3. The mean of the synaptic weights in each of the four quarters for Fig. 12.

group 1: pair 1 (higher μ) group 2: pair 5 (lower μ)	mean weights ($\mu\text{A}/\text{cm}^2$)		standard error
	theory	simulation	
higher \rightarrow higher (top-left)	0.025	0.025	0.00022
lower \rightarrow higher (top-right)	0.020	0.020	0.00019
higher \rightarrow lower (bottom-left)	0.028	0.028	0.00023
lower \rightarrow lower (bottom-right)	0.025	0.025	0.00022

3.4. Networks of identical neurons

Under fixed baseline firing rate, the spiking cross-covariance can still affect the evolution of the network structure, even for the STDP rule such that the second part of Eq. (2.7) is non-zero. The potentiation dominated Hebbian STDP rule is

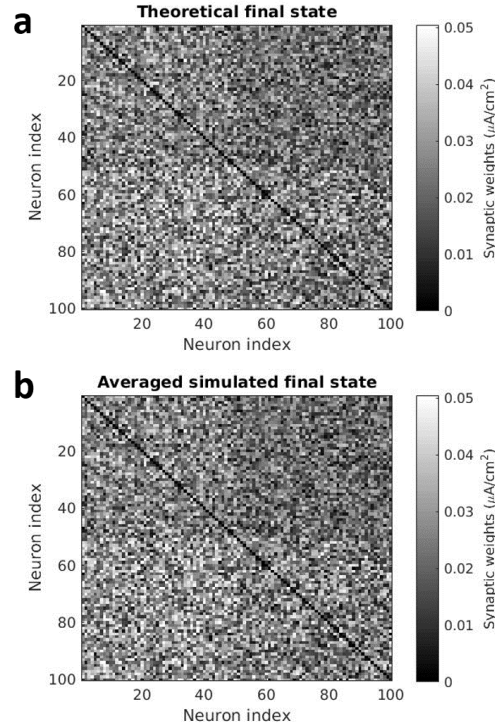


Figure 12. The synaptic weight matrices for the final state of the network under balanced Anti-Hebbian STDP. (a) The synaptic weight matrix for the final state obtained by theory. **(b)** The synaptic weight matrix for the final state obtained by averaging 10 numerical simulations.

applied for the networks by setting $f_+ = A \cdot f_-$ and $\tau_+ = \tau_-$ with $A > 1$. For this case, $f_+ \tau_+ - f_- \tau_- > 0$. Similar to the previous section, the phase planes for two-cell recurrent networks (Fig. 6a) under potentiation dominated Hebbian STDP ($A = 1.5$) are analyzed firstly. The two neurons are identical from the same network by applying the parameter setting in Table 1.

There are three stable fixed points: $(\mathbf{W}_{21}, \mathbf{W}_{12}) = (5, 0)$, $(0, 5)$ and $(5, 5)$ in the phase planes (Fig. 14). However, the areas of the basin of attraction of each stable fixed point are different between networks. The basin of attraction of the stable fixed point $(\mathbf{W}_{21}, \mathbf{W}_{12}) = (5, 5)$ is larger for the network with neurons of lower μ (Fig. 14b) than that for the network with neurons of higher μ (Fig. 14a). This means more synaptic weights will be potentiated for network of neurons with lower background input mean. Thus, we can make a prediction that, for multiple large networks with the same initial structure, the same baseline firing rate for each neuron but different background input, more synaptic weights of the network with lower background input mean (μ) will be potentiated under potentiation dominated Hebbian STDP.

Two networks of 100 cells with the same initial synaptic weight matrix are considered as previous section (Fig. 8). All the 100 neurons of the first network have parameter setting 1 in Table 1 while the neurons of the second network have parameter setting 5. This makes sure that the neurons from these two networks have the same baseline firing rate. Then the potentiation dominated STDP rule

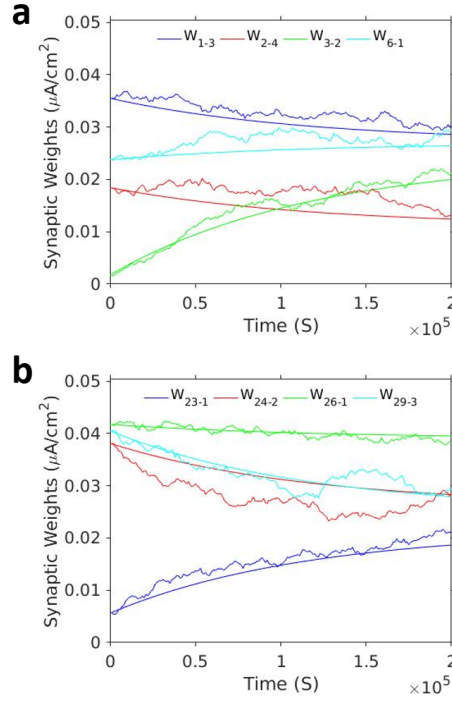


Figure 13. The evolution of selected synaptic weights in the 100-cell network under balanced Anti-Hebbian STDP. Corresponding to Fig. 12. (a, b) The smooth curves are got from theory, while the jagged curves are obtained by averaging 10 simulated realizations.

($f_+ = 1.005 \cdot f_-$) is applied for them.

After training by the learning rule, the synaptic weight matrices (Fig. 15) and the evolution for each synaptic weights (Fig. 16) are obtained. Although this is not very obvious, there are more white dots in synaptic weight matrices for the network with parameter setting 5 (Fig. 15c and d) than those for the network with parameter setting 1 (Fig. 15a and b). This means that the network of neurons with lower μ have more potentiated synaptic weights. This difference is illustrated clearly through calculating the means of these synaptic weight matrices (Table 4).

Table 4. The mean of the synaptic weight matrices for Fig. 15.

Network parameter setting	mean weights ($\mu\text{A}/\text{cm}^2$)		standard error
	theory	simulation	
Setting 1	0.030	0.030	0.00021
Setting 5	0.033	0.033	0.00019

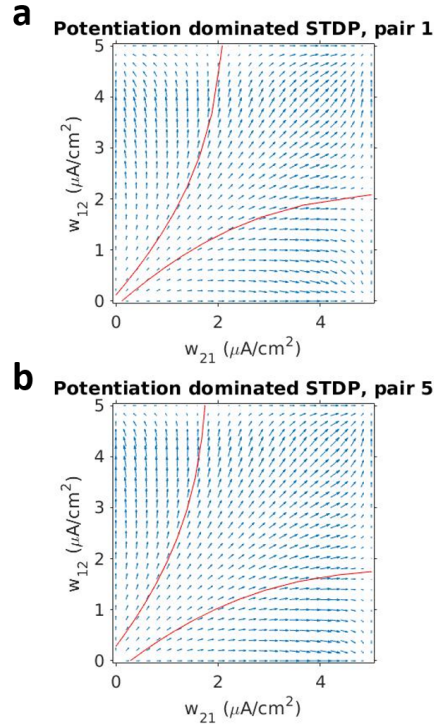


Figure 14. Phase planes for synaptic weights in two-cell recurrent networks under potentiation dominated STDP rule. (a) Phase plane for both neurons with parameter setting 1. **(b)** Phase plane for both neurons with parameter setting 5.

4. Discussion

In this paper, a self-consistent framework is provided to study the effect of the correlated spiking activity and STDP learning rules on the structures of recurrent networks composed of EIF neurons. For fixed baseline firing rate, the background input plays an important role in the shapes of spiking cross-covariance and the evolution of network structure (Fig. 6): higher input mean leads to bigger amplitude of covariance and faster modification of synaptic weights. The analysis of the phase planes of simple two-cell recurrent networks gives some insights about the structures of large networks. For the fixed baseline firing rate of all neurons in one network, the connections from neurons with lower background input mean to those with higher are more likely to strengthen under balanced Hebbian STDP rule. The opposite conclusion holds for balanced Anti-Hebbian STDP case. In addition, for networks of identical neurons with the same fixed baseline firing rate but different background input among networks, there are more potentiated connections under potentiation dominated STDP in the network with lower background input mean.

The linear response theory for approximating the spiking cross-covariance of Lindner et al. [31] was generalized by Trousdale et al. [47] by accounting for the length of directed chains of neurons along with higher order corrections. Trousdale et al. focused on the impact of network structure on spiking covariance, without considering the plasticity of networks. Our work extends theirs to show that

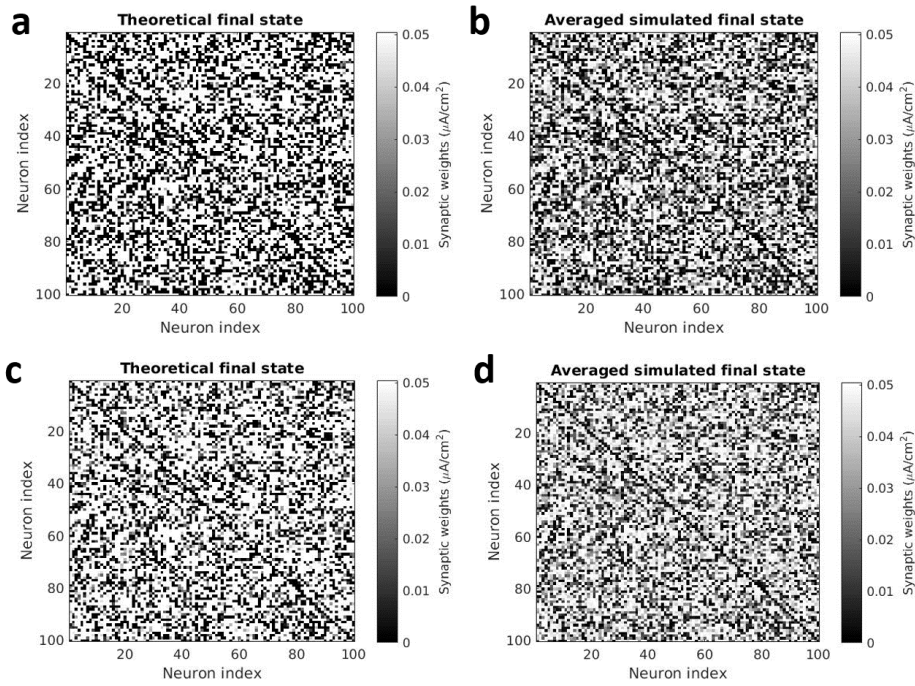


Figure 15. The synaptic weight matrices for 100-cell networks after being trained by potentiation dominated STDP. (a) Theoretical synaptic weight matrix for the network with parameter setting 1. (b) Averaged simulated (by 10 realizations) synaptic weight matrix for the network with parameter setting 1. (c) Theoretical synaptic weight matrix for the network with parameter setting 5. (d) Averaged simulated (by 10 realizations) synaptic weight matrix for the network with parameter setting 5.

correlated spiking activity can also affect the network structure under STDP. Correlated activities between neurons and network structure affect each other due to the dynamic property of networks.

This study is closely related to that of Babadi and Abbott [5], who also analyzed pairwise interactions of neurons affected by STDP. Both studies present the approach for inferring the structures in large networks from the analysis of simple circuits of neurons. However, they assumed that the input to each neuron was Poisson-like so that the model can be simplified. This allowed them to perform a detailed analytic study on how STDP affects the synapses between the two neurons, but lost some intrinsic properties of actual neurons and networks. Their conclusions are based on different baseline firing rates and STDP rules. Here, without such an assumption, their results are generalized for networks of EIF neurons with the same baseline firing rate by taking the background input and correlated spiking activity into account.

The work is also comparable with Pernice et al. [36], who examined the correlation structure in networks of interacting Hawkes processes. Their studies represent correlations between neuron pairs in terms of contributions of different connectivity motifs. Our methods, however, are different because Pernice et al. did not compare their results to those obtained using physiological models and did not take

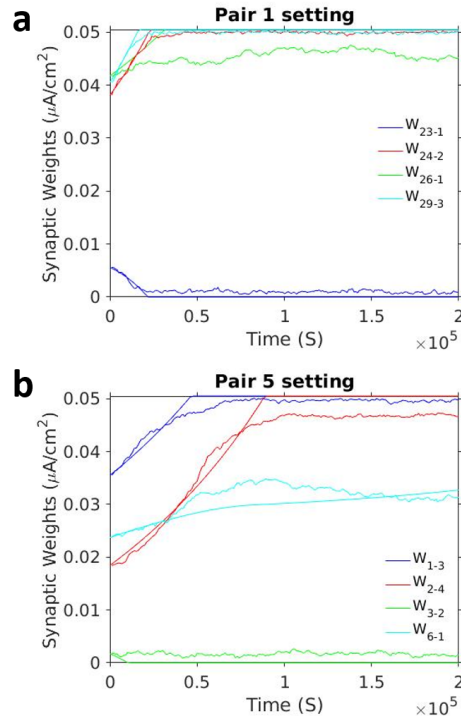


Figure 16. The evolution of selected synaptic weights in the 100-cell networks under potentiation dominated Hebbian STDP. Corresponding to Fig. 15. (a) For network of identical neurons with parameter setting 1. (b) For network of identical neurons with parameter setting 5.

into account the response characteristics of individual neurons, even though their expressions are accurate for Hawkes processes. Furthermore, for simplicity Pernice et al. analyzed only total spike count covariances, which were the integrals of the cross-correlation functions. Similarly, Toyozumi et al. [46] derived expressions for cross-correlations in networks of interacting point process models in the Generalized Linear Model (GLM) class. Although they shared many characteristics with Hawkes processes, they also had a static nonlinearity that shaped the spike emission rate.

The framework and approach developed in this paper can be applied for further research. For instance, how external input affect the network structures under STDP [16–19]. Moreover, there are more detailed and physiologically realistic neuron models than EIF neuron model, such as Connor-Stevens neuron model [9], which can spike automatically without setting a threshold. Our methods may be extended to analyze such neuron models. In addition, besides STDP with paired spikes, people also consider triplet STDP learning rule [22]. It will be an interesting topic about the impact of triplet STDP on network structure by applying our methods. We hope this tool will contribute to a better understanding of the evolution of network structure with more realistic neuron models, more structured input and more complex learning rules.

Acknowledgements

We thank Professor Krešimir Josić for the helpful discussions and guidance.

References

- [1] L. F. Abbott and S. B. Nelson, *Synaptic plasticity: taming the beast*, Nature Neuroscience, 2000, 3(11s), 1178–1183.
- [2] C. Allen and C. F. Stevens, *An evaluation of causes for unreliability of synaptic transmission*, Proc. Natl. Acad. Sci., 1994, 91(22), 10380–10383.
- [3] C. B. Allen, T. Celikel and D. E. Feldman, *Long-term depression induced by sensory deprivation during cortical map plasticity in vivo*, Nature Neuroscience, 2003, 6(3), 291–299.
- [4] B. Babadi and L. F. Abbott, *Intrinsic stability of temporally shifted spike-timing dependent plasticity*, PLoS Computational Biology, 2010, 6(11), e1000961. doi:10.1371/journal.pcbi.1000961.
- [5] B. Babadi and L. F. Abbott, *Pairwise analysis can account for network structures arising from spike-timing dependent plasticity*, PLoS Comput Biol, 2013, 9(2), e1002906. doi: 10.1371/journal.pcbi.1002906.
- [6] L. Badel, S. Lefort, T. K. Berger et al., *Extracting non-linear integrate-and-fire models from experimental data using dynamic $i-v$ curves*, Biological Cybernetics, 2008, 99(4-5), 361–370.
- [7] G.-q. Bi and M.-m. Poo, *Synaptic modifications in cultured hippocampal neurons: dependence on spike timing, synaptic strength, and postsynaptic cell type*, Journal of Neuroscience, 1998, 18(24), 10464–10472.
- [8] C. Clopath, L. Büsing, E. Vasilaki and W. Gerstner, *Connectivity reflects coding: a model of voltage-based STDP with homeostasis*, Nature Neuroscience, 2010, 13(3), 344–352.
- [9] J. Connor and C. Stevens, *Prediction of repetitive firing behaviour from voltage clamp data on an isolated neurone soma*, The Journal of Physiology, 1971, 213(1), 31–53.
- [10] C. W. Dickey, A. Sargsyan, J. R. Madsen et al., *Travelling spindles create necessary conditions for spike-timing-dependent plasticity in humans*, Nature communications, 2021, 12(1), 1–15.
- [11] B. Doiron, B. Lindner, A. Longtin et al., *Oscillatory activity in electrosensory neurons increases with the spatial correlation of the stochastic input stimulus*, Phys Rev Lett, 2004, 93(4), 048101.
- [12] R. Falcón-Moya, M. Pérez-Rodríguez, J. Prius-Mengual et al., *Astrocyte-mediated switch in spike timing-dependent plasticity during hippocampal development*, Nature communications, 2020, 11(1), 1–14.
- [13] N. Fourcaud-Trocme, D. Hansel, C. Van Vreeswijk and N. Brunel, *How spike generation mechanisms determine the neuronal response to fluctuating inputs*, Journal of Neuroscience, 2003, 23(37), 11628–11640.
- [14] C. Gardiner, *Stochastic Methods: A Handbook for the Natural and Social Sciences*, Springer, Berlin Heidelberg, 2009.

- [15] W. Gerstner, R. Kempter, J. L. van Hemmen and H. Wagner, *A neuronal learning rule for sub-millisecond temporal coding*, Nature, 1996, 383(6595), 76.
- [16] M. Gilson, A. N. Burkitt, D. B. Grayden et al., *Emergence of network structure due to spike-timing-dependent plasticity in recurrent neuronal networks. i. input selectivity-strengthening correlated input pathways*, Biological Cybernetics, 2009, 101(2), 81–102.
- [17] M. Gilson, A. N. Burkitt, D. B. Grayden et al., *Emergence of network structure due to spike-timing-dependent plasticity in recurrent neuronal networks. ii. input selectivity-symmetry breaking*, Biological Cybernetics, 2009, 101(2), 103–114.
- [18] M. Gilson, A. N. Burkitt, D. B. Grayden et al., *Emergence of network structure due to spike-timing-dependent plasticity in recurrent neuronal networks iii: Partially connected neurons driven by spontaneous activity*, Biological Cybernetics, 2009, 101(5-6), 411–426.
- [19] M. Gilson, A. N. Burkitt, D. B. Grayden et al., *Emergence of network structure due to spike-timing-dependent plasticity in recurrent neuronal networks iv: structuring synaptic pathways among recurrent connections*, Biological Cybernetics, 2009, 101(5-6), 427–444.
- [20] M. Gilson, A. N. Burkitt, D. B. Grayden et al., *Emergence of network structure due to spike-timing-dependent plasticity in recurrent neuronal networks v: self-organization schemes and weight dependence*, Biological Cybernetics, 2010, 103(5), 365–386.
- [21] M. Gilson, A. N. Burkitt and J. L. Van Hemmen, *STDP in recurrent neuronal networks*, Frontiers in Computational Neuroscience, 2010, 4, 23. doi: 10.3389/fncom.2010.00023.
- [22] J. Gjorgjieva, C. Clopath, J. Audet and J.-P. Pfister, *A triplet spike-timing-dependent plasticity model generalizes the bienerstock-cooper-munro rule to higher-order spatiotemporal correlations*, Proceedings of the National Academy of Sciences, 2011, 108(48), 19383–19388.
- [23] R. Gütiğ, R. Aharonov, S. Rotter and H. Sompolinsky, *Learning input correlations through nonlinear temporally asymmetric hebbian plasticity*, Journal of Neuroscience, 2003, 23(9), 3697–3714.
- [24] E. M. Izhikevich, J. A. Gally and G. M. Edelman, *Spike-timing dynamics of neuronal groups*, Cerebral Cortex, 2004, 14(8), 933–944.
- [25] V. Jacob, D. J. Brasier, I. Erchova et al., *Spike timing-dependent synaptic depression in the in vivo barrel cortex of the rat*, Journal of Neuroscience, 2007, 27(6), 1271–1284.
- [26] R. Jolivet, A. Rauch, H.-R. Lüscher and W. Gerstner, *Integrate-and-fire models with adaptation are good enough: predicting spike times under random current injection*, Advances in neural information processing systems, 2006, 18, 595–602.
- [27] R. Kempter, W. Gerstner and J. L. v. Hemmen, *Intrinsic stabilization of output rates by spike-based hebbian learning*, Neural Computation, 2001, 13(12), 2709–2741.
- [28] R. Kempter, W. Gerstner and J. L. Van Hemmen, *Hebbian learning and spiking neurons*, Physical Review E, 1999, 59(4), 4498.

- [29] J. Kozloski and G. A. Cecchi, *A theory of loop formation and elimination by spike timing-dependent plasticity*, Front Neural Circuits, 2010, 4, 7. doi: 10.3389/fncir.2010.00007.
- [30] B. Lindner, *Coherence and stochastic resonance in nonlinear dynamical systems*, Logos-Verlag, 2002.
- [31] B. Lindner, B. Doiron and A. Longtin, *Theory of oscillatory firing induced by spatially correlated noise and delayed inhibitory feedback*, Phys Rev E, 2005, 72(6), 061919.
- [32] E. V. Lubenov and A. G. Siapas, *Decoupling through synchrony in neuronal circuits with propagation delays*, Neuron, 2008, 58(1), 118–131.
- [33] A. Morrison, A. Aertsen and M. Diesmann, *Spike-timing-dependent plasticity in balanced random networks*, Neural Computation, 2007, 19(6), 1437–1467.
- [34] G. K. Ocker, A. Litwin-Kumar and B. Doiron, *Self-organization of microcircuits in networks of spiking neurons with plastic synapses*, PLoS Comput Biol, 2015, 11(8), e1004458.
- [35] A. Payeur, J. Guerguiev, F. Zenke et al., *Burst-dependent synaptic plasticity can coordinate learning in hierarchical circuits*, Nature neuroscience, 2021, 1–10.
- [36] V. Pernice, B. Staude, S. Cardanobile and S. Rotter, *How structure determines correlations in neuronal networks*, PLoS computational biology, 2011, 7(5), e1002059.
- [37] A. Rauch, G. La Camera, H.-R. Lüscher et al., *Neocortical pyramidal cells respond as integrate-and-fire neurons to in vivo-like input currents*, Journal of Neurophysiology, 2003, 90(3), 1598–1612.
- [38] A. Renart, N. Brunel and X. Wang, *Mean-field theory of irregularly spiking neuronal populations and working memory in recurrent cortical networks*, Computational Neuroscience: A comprehensive approach, 2004, 431–490.
- [39] M. J. Richardson, *Firing-rate response of linear and nonlinear integrate-and-fire neurons to modulated current-based and conductance-based synaptic drive*, Physical Review E, 2007, 76(2), 021919.
- [40] M. J. Richardson, *Spike-train spectra and network response functions for nonlinear integrate-and-fire neurons*, Biol Cybern, 2008, 99(4-5), 381–392.
- [41] M. N. Shadlen and W. T. Newsome, *The variable discharge of cortical neurons: implications for connectivity, computation, and information coding*, Journal of Neuroscience, 1998, 18(10), 3870–3896.
- [42] S. Song and L. F. Abbott, *Cortical development and remapping through spike timing-dependent plasticity*, Neuron, 2001, 32(2), 339–350.
- [43] S. Song, K. D. Miller and L. F. Abbott, *Competitive hebbian learning through spike-timing-dependent synaptic plasticity*, Nature Neuroscience, 2000, 3(9), 919.
- [44] C. F. Stevens and A. M. Zador, *When is an integrate-and-fire neuron like a poisson neuron?*, Advances in neural information processing systems, 1996, 103–109.

- [45] S. Tazerart, D. E. Mitchell, S. Miranda-Rottmann and R. Araya, *A spike-timing-dependent plasticity rule for dendritic spines*, Nature communications, 2020, 11(1), 1–16.
- [46] T. Toyozumi, K. R. Rad and L. Paninski, *Mean-field approximations for coupled populations of generalized linear model spiking neurons with markov refractoriness*, Neural computation, 2009, 21(5), 1203–1243.
- [47] J. Trousdale, Y. Hu, E. Shea-Brown and K. Josić, *Impact of network structure and cellular response on spike time correlations*, PLoS Computational Biology, 2012, 8(3), e1002408.
- [48] M. Udakis, V. Pedrosa, S. E. Chamberlain et al., *Interneuron-specific plasticity at parvalbumin and somatostatin inhibitory synapses onto ca1 pyramidal neurons shapes hippocampal output*, Nature communications, 2020, 11(1), 1–17.
- [49] M. C. Van Rossum, G. Q. Bi and G. G. Turrigiano, *Stable hebbian learning from spike timing-dependent plasticity*, Journal of Neuroscience, 2000, 20(23), 8812–8821.
- [50] E. Vickers, D. Osypenko, C. Clark et al., *LTP of inhibition at PV interneuron output synapses requires developmental BMP signaling*, Scientific Reports, 2020, 10(1), 1–12.
- [51] J. A. White, J. T. Rubinstein and A. R. Kay, *Channel noise in neurons*, Trends in Neurosciences, 2000, 23(3), 131–137.
- [52] L. I. Zhang, H. W. Tao, C. E. Holt et al., *A critical window for cooperation and competition among developing retinotectal synapses*, Nature, 1998, 395(6697), 37–44.